JOURNAL OF PROPULSION AND POWER
Vol. 23, No. 3, May–June 2007

Online Vibration Monitoring of Ball Bearing Damage Using an Experimental Test Rig

Fred K. Choy*
University of Akron, Akron, Ohio 44325-3903
Lei Wang.†
The Timken Company, Canton, Ohio 44706
and
Jianyou Zhou‡ and Minel J. Braun*
University of Akron, Akron, Ohio 44325-3903

DOI: 10.2514/1.18180

Rolling element bearings in rotating machinery are vulnerable mechanical components that are prone to premature failure with dire consequences. Early warning of impending bearing failures is vital to the safety and reliability of high-speed turbomachinery. At present, vibration monitoring is one of the most common procedures used to detect online damage and early failure of rolling element bearings. This paper presents results from an experimental rotor-bearing test rig with known induced damage in the supporting ball bearings. Two types of damages are examined, namely, that of 1) the ball rolling element and 2) the inner race of the bearing. Four online vibration signature analyzing schemes are used: 1) time averaging, 2) frequency domain analysis, 3) joint time-frequency analysis (Wigner–Ville and wavelet transforms), and 4) chaotic vibration analysis (modified Poincaré diagrams). The results from the various procedures are compared for efficiency in early pinpointing of damage and reliability in the detection. Based on this study, it was found that, in the case of race damage in which interactions with the damage area take place in a periodic manner during shaft rotation, vibration signals resulting from contacts with the damage location can generally be found within a typical window of data sampling, and damage can be identified using all four selected online procedures. For the case of ball-element damage, the vibration signals are chaotic in nature due to the unpredictable rotational patterns of the ball elements. Under such conditions, interactions with the ball-element damage area may not occur within the particular data sampling period, and as a result, damage cannot be detected by the traditional time-frequency procedures. It is also demonstrated that, in this study, the modified Poincaré map approach using a relatively large amount of sampling data can be effective in identifying damage in the ball rolling element.

Nomenclature

a, b	=	scale and shift parameters used in wavelet transform
$\mathrm{CWT}_f(a, b)$	=	continuous wavelet transform
f	=	frequency, Hz
j	=	imaginary part of a complex number
$x(f)$	=	frequency domain signal after FFT
$x(t)$	=	time domain signal
$x^*(t)$	=	complex conjugate of time signal
t	=	time, s
$W_x(t, f)$	=	Wigner–Ville distribution of time signal
τ	=	time domain variable
$\psi_{a,b}(t)$	=	wavelet function

I. Introduction

IN THE rotating machinery industry, in which both weight-to-load factor and efficiency are pushed to their design limits, one of the major concerns is the fatigue failure in rolling element bearing components. Such failures often result from excessive wear in rolling-ball elements as well as damage/wear of the inner/outer races of the bearing. At present, rolling element bearings are significant contributors to both flight safety incidents and maintenance costs, especially in the aeronautics and aerospace industries. In the last 20 years, bearing replacement has composed almost 30% of the maintenance costs in the aircraft industry. Current onboard condition monitoring systems often fail to provide sufficient time between warning and failure so that timely safety measures can be taken. At times, a small fault in the bearing system can quickly develop into a dangerous failure mode without any notable signs. In addition, inaccurate interpretation of operational conditions may result in false alarms and unnecessary repairs and downtime.

For preventing unexpected failure in rolling element bearing systems, some work [1–3] has been carried out based on a statistical model developed by Lundberg and Palmgren [3] using reliability models based on classical fatigue theory and the Weibull failure distribution. However, most of this work does not consider the conditions of the machine components and their operating environments during various phases of their lifespan. Today, signature analysis of machine vibration/acoustic signals [4–9] is one of the advanced fault identification procedures used in high-speed rotor-bearing systems. Besides the traditional approaches using time signal and frequency spectrum analysis that have gained considerable success, a joint time-frequency domain method, based on the Wigner–Ville distribution, was recently applied by the authors [5–7] to detect gear and bearing failures in a transmission system. The joint time-frequency domain method provides an instantaneous frequency spectrum of the system at various points of the rotation of the shaft. In addition, this paper also applies the wavelet method [10,11] to examine vibration data. Although these two joint time-frequency methods are mostly used separately, their combined application can sometimes provide accurate pinpointing of system failures and their severities.

Received 13 June 2005; revision received 2 May 2006; accepted for publication 3 May 2006.

*Professor, Department of Mechanical Engineering.
†Formerly with B&C Engineering, Inc., Akron, Ohio.
‡Graduate Student, Department of Mechanical Engineering.

Even though the use of chaotic vibration analysis was first performed by Ehrich [12] in the early seventies, its full application in identifying and quantifying ball bearing damage has not been fully realized. As the ball element is rotating freely in all directions, the interactions with the damaged ball element with the bearing races can be quite chaotic, resulting in a highly nonperiodic type of vibration signature. Using the statistical approach developed through chaotic vibration analysis, the modified Poincaré map applied in this study identifies and quantifies damage in bearings based on the acquired experimental data. A complete discussion of the usage of the modified Poincaré map and the other existing methods is also presented in this paper.

II. Description of the Experimental Study

The study of damage identification and remaining life prognosis for a ball bearing is carried out with a high-speed test rig. All eight ball-element bearings used in this study have the following characteristics:

1) Bearing o.d. is 1.85 in.
2) Bearing i.d. is 0.625 in.
3) Bearing length is 0.625 in.
4) Ball diameter is 0.2813 in.
5) Pitch diameter is 1.1228 in.
6) Train frequency is 0.375.
7) Ball pass frequency to the outer race is 3.
8) Ball pass frequency to the inner race (shaft speed) is 5.

During the test, the ball bearing on the driving electric motor side was kept intact while the bearing on the belt side was changed for three different cases of study: 1) with an undamaged eight-ball bearing, 2) with a bearing damaged at the inner race (Fig. 1), and 3) with a bearing having one of the eight ball elements damaged (Fig. 2).

The measured damage profiles are given in 3-D form in both Figs. 1b and 2b (with accuracy of measurement of 0.0001 in.). The shaft speed is set at 80 Hz (4800 rpm was found to be the optimal speed for constant speed operation of the electric motor based on its size) and vibration data is obtained through a set of x- and y-direction accelerometers positioned at the bearing supports of the damaged bearing. The data is then transmitted to a PC-based 12-bit high-speed analog-to-digital data acquisition system. With accelerometer sensitivity of 10 g/V and digital conversion settings of -10 to $+10$ V, the accuracy of measurement is estimated to be within 0.005 V (0.05 g). Both shaft speed and bearing ball cage speed are also measured using optical encoders. The sampling rate of the vibration data is set to 375 samples per revolution of the shaft, as determined by the optical encoder. Vibration signals for approximately 2000 revolutions are acquired during a typical window sampling time and stored for fault identification vibration signature analysis.

Fig. 1 Inner race damage: a) photo, b) profile.

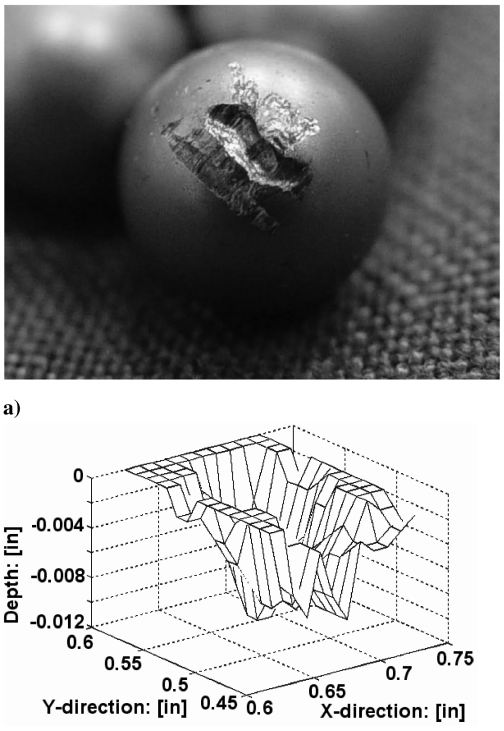

Fig. 2 Ball-element damage: a) photo, b) profile.

III. Vibration Signature Analysis Procedures

To provide for an accurate identification of the faulty bearing components, four major vibration signature analysis procedures are used: 1) the frequency spectral analysis, 2) the Wigner–Ville distribution (WVD), 3) the wavelet transform, and 4) the chaotic vibration-based modified Poincaré map.

The frequency spectral analysis is based on the numerical FFT transform on the original time signal to provide an average estimation of the excited frequency components during the period of sampling used in the analysis. Because a 1024-point transform is used in this study, the length of the sampling time window period is relatively short and covers only two revolutions of the shaft. (1024 points sampling at 30,000 Hz equals to 0.034 s of acquired data, which corresponds to less than three revolutions of the shaft rotating at 80 Hz.) Thus the results can sometimes be nonconclusive due to the chaotic motion or rotation of the damaged rolling element (damaged locations in the rolling element may not make contact with the inner/outer race during the short period of operations). Frequency spectra from data sampling windows at different times have been added to provide a more accurate representation of the vibration signature of the system.

The WVD is a time-frequency decomposition that provides a 3-D (time, frequency, amplitude) representation of an input signal, which is well-suited for describing transient or other nonstationary phenomena. It provides an instantaneous display of the frequency components at each time instant within the sampling time window period, which is not available in standard Fourier spectral analysis. In other words, the WVD is capable of detecting any instantaneous

amplitude and phase change of the vibration signals during the short data sampling time period. In the time domain, the WVD distribution is defined as [4–9]

$$W_x(t,f) = \int_{-\infty}^{\infty} x(t+\tau/2)x^*(t-\tau/2)\exp(-j2\pi f\tau)\,\mathrm{d}\tau \qquad (1)$$

where $x(t)$ is restricted to a complex continuous time analytic signal with a Fourier transform $x(f)$.

The wavelet transform provides a time-frequency (specifically time-scale) analysis of an input signal [10,11]. Similar to the WVD in this respect, it has an advantage over the Fourier transform, in that it can indicate the frequencies that are present in a signal but cannot determine at what times those frequencies are present. The wavelet transform has the advantage over the WVD in that it is linear in its application. The WVD, because of its inherent nonlinearity, produces interference terms that introduce nonzero values into the WVD at unexpected locations of the time-frequency plane. These interference terms for the WVD can make it difficult to correctly analyze a signal.

The continuous wavelet transform [10,11] of input signal $x(t)$ is defined as

$$\mathrm{CWT}_f(a,b) = \frac{1}{\sqrt{a}}\int_R x(t)\psi\left(\frac{t-b}{a}\right)\mathrm{d}t \qquad (2)$$

where $a \in R^+$ is the scale and $b \in R$ is the shift parameter. The factor $\frac{1}{\sqrt{a}}$ is used to conserve energy. The fundamental operations applied in this definition are scaling and shifting the particular wavelet function used in the integrand. Then the integral measures the similarity between the signal $x(t)$ and the shifts and scales of the wavelet function $\psi_{a,b}(t)$, where

$$\psi_{a,b}(t) = \frac{1}{\sqrt{a}}\psi\left(\frac{t-b}{a}\right) \qquad (3)$$

The use of chaotic theory in analyzing damage problems in rotating machinery for nonsynchronous vibration components is first performed in detail by Ehrich [12]. The chaotic dynamics of the system due to damage in the ball element is quite similar to the contact problem in its nonrepeatable nature. As the ball element is allowed to rotate freely in all directions, the contact of the damaged location on the ball with the inner or outer races can be quite chaotic, resulting in a highly nonperiodic type of vibration signature. Using the statistical approach developed in chaotic vibration analysis, the Poincaré map, the average phase and amplitude of vibration at a certain point on the shaft over a number of periodic time can be determined by averaging the vibrations measured at the particular point every time after a complete revolution (complete revolution of the shaft or the cage). Applying this procedure repeatedly to different points on the shaft over a large number of revolutions, a dependable statistical representation of the shaft vibration signature for each shaft/cage position can be determined. Normalizing vibration amplitudes in both x- and y-directions, a modified Poincaré map of the vibration signals can be constructed. The results and applications of this modified Poincaré map will be given in detail in the next section.

IV. Discussion of Results

To study the dynamic characteristics of the experimental test rig, frequency response functions of the system are evaluated from the results based on impact hammer applications. Results of the frequency excitation functions for both the x- and y-directions are given in Figs. 3a and 3b, respectively. In the x direction, a major response frequency is excited at 3000 Hz with some sideband excitations at around 2300 Hz and 3500 Hz or higher. Comparing Fig. 3a with Fig. 3b, it is found that the major frequency has shifted to approximately 3200 Hz due to the variations in the x- and y-supporting stiffness. As the loading is applied in the y direction, the amplitudes of frequencies excited in the x direction are generally higher than those in the y direction. Based on this result, the vibration analysis will be predominantly performed on data collected by the x-direction accelerometer.

To perform an overall vibration signature analysis of the system due to damage/wear in the bearing, vibration data from accelerometers are collected for cases 1) with no bearing damage, 2) with damage at the inner race, and 3) with damage in the ball element, (see damage pictures in Figs. 1 and 2). The vibration signals from the accelerometers for each of the three cases mentioned are acquired at two different time windows to demonstrate the chaotic nature of some of the vibration results. Typical results acquired from two separate time windows for the three cases of study are shown in Fig. 4. Note that there are only slight differences between the time signals collected at different times for case 1 with no damage (Figs. 4a and 4b) and case 2 with inner race damage (Figs. 4c and 4d). However, the two time vibration signals for case 3 with ball-element damage (Figs. 4e and 4f) show substantial differences due to the chaotic rotational motion of the ball element ensuing contact between the ball element and the inner/outer races of the bearing. Figure 5 depicts the frequency spectra of the three cases of study. For case 1 (Fig. 5a), there is practically no excited frequency component at the system's natural frequency of 3000 Hz. Only a very small frequency component can be detected at the ball pass frequency of 640 Hz (eight ball bearings rotating at 80 Hz). For case 2 (Fig. 5b), large frequency components around the system's natural frequency appear in the frequency range of 2300–3000 Hz. Large frequency components are also found between 1500 and 2000 Hz, seemingly due to the excitation of secondary natural frequencies at multiples (three and four times) of the ball passing the frequency of 640 Hz. Figure 5c shows the frequency spectrum of the vibration signal due to ball-element damage, (case 3), corresponding to the time signal acquired in time window 1, as shown in Fig. 4e. In this case only very small frequency components at multiples of the shaft speed and the ball pass frequency can be seen in the spectrum, similarly to the case

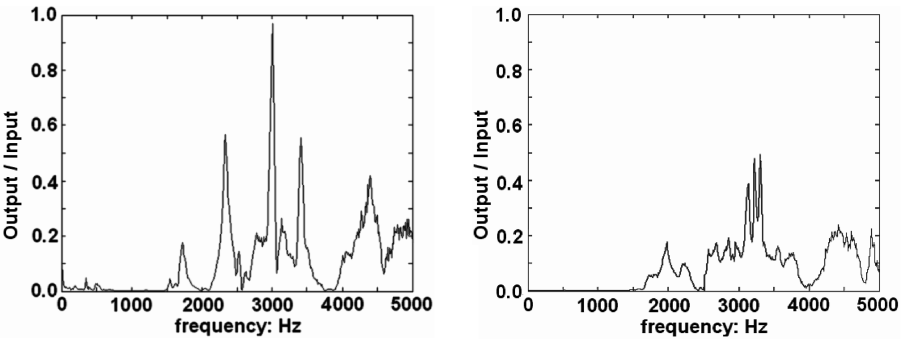

Fig. 3 System frequency excitation using an impact hammer: a) x direction, b) y direction.

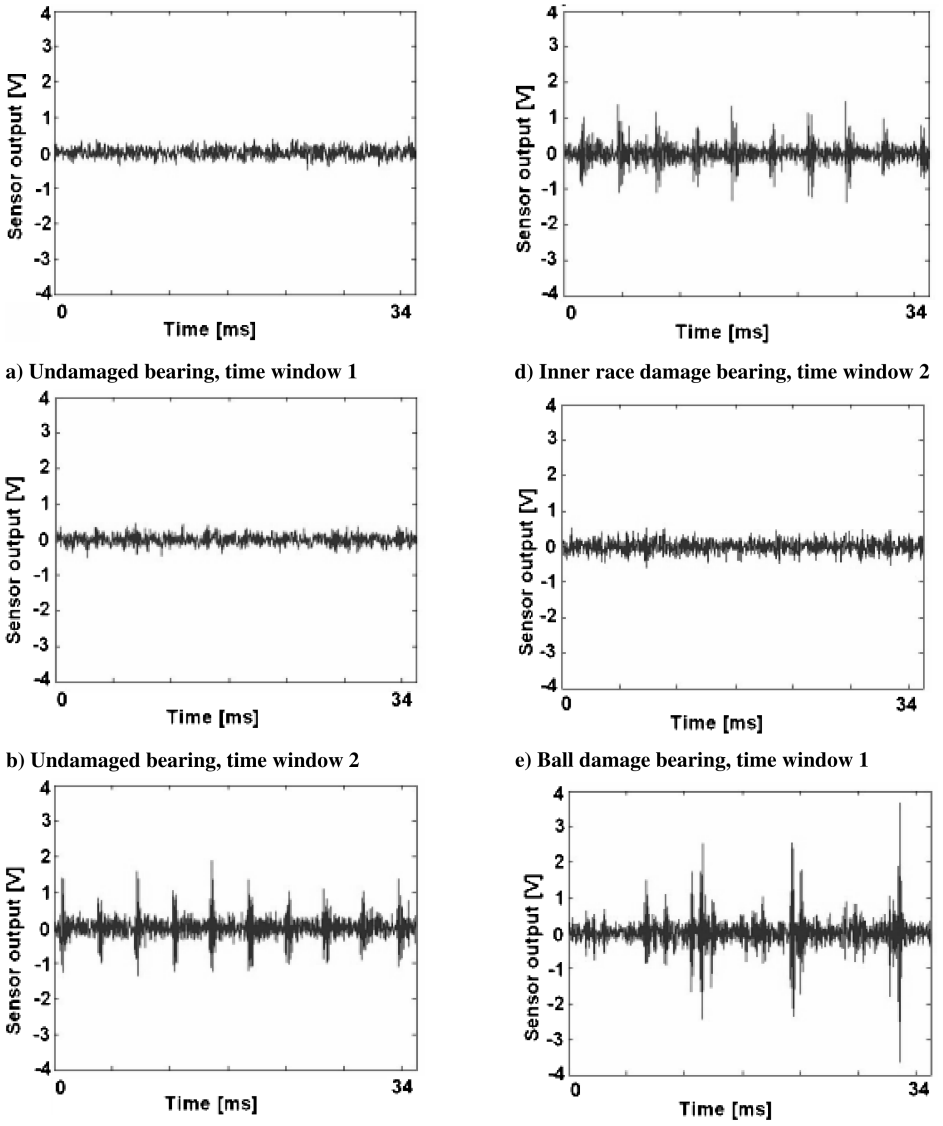

a) Undamaged bearing, time window 1

d) Inner race damage bearing, time window 2

b) Undamaged bearing, time window 2

e) Ball damage bearing, time window 1

c) Inner race damage bearing, time window 1

f) Ball damage bearing, time window 2

Fig. 4 Time signals for different bearings at time windows 1 and 2.

with no damage (Fig. 5a). The damage cannot be detected in this time period because the sampling time window did not "catch" a contact event between the chaotically rotating balls and the races. However, the frequency spectrum (Fig. 5d) resulting from the other vibration signal window shown in Fig. 4f shows large frequency components near the 3000 Hz region with a sizable vibration component at the ball pass frequency of 640 Hz. In this case the sampling window is sufficient to register the interactions between the damaged ball and the races. However, aside from indicating the slight shifting of the excited frequencies, the analysis still does not provide a definite identification of the type of bearing damage.

We can now proceed to show the results of two other time-frequency procedures, the WVD and the wavelet transform, as they are applied to the same four sets of time data shown in Fig. 5. One can see that in the WVD representation (the vibration amplitude is represented by color/gray scale with the darkest color related to a fixed maximum amplitude for comparison purposed, the time-scale for one revolution of the shaft is along the vertical axis, and the corresponding frequency spectrum is on the horizontal axis) for the case 1, Fig. 6a does not show any particular features for bearing damage. For case 2, the WVD results (Fig. 6b) show the formation of a long hollow diamondlike cross pattern, which indicates a short term phase change in the time signal as the ball element rolls over the damaged inner race portion of the bearing [9]. For case 3 when the ball element is damaged, the WVD indicates in Fig. 6d a short solid diamondlike cross pattern, representing the existence of a short-term increase in amplitude (burst) [9]. Such a burst effect is due to a sudden change in the overall bearing stiffness when the damaged portion of the ball element makes contact with the inner/outer race of the bearing. (The position for the location of the ball-element damage, with reference to the 360 deg of shaft rotation in the vertical time axis, is adjusted to be in the same position as the inner race damage for comparison purposes.) Based on the results from this study using the previously developed pattern recognition schemes [9], one can conclude that WVD is not only capable of pinpointing the damage and its location, it can also, in some degrees, identify the types existing bearing damage. Although the WVD gray scale provides relative magnitudes of the vibration components, in this case, only limited information can be extracted concerning the level of damage. To further examine the damage in the bearing, a wavelet transform procedure is applied to the vibration signals. The Db3 of the Daubechies family [10,11] of wavelets are selected due to their similarity to the pattern of the time signal at the damaged location. A scaling factor of 3 to 100 is chosen for an output frequency range of 200–6666 Hz. Figures 7a and 7c represent, respectively, the wavelet transform for case 1 with no damage (Fig. 5a) and case 3 with no contact between the damaged ball and the race (Fig. 5c). Note that for both cases, there are very few vibration amplitudes in the plot to

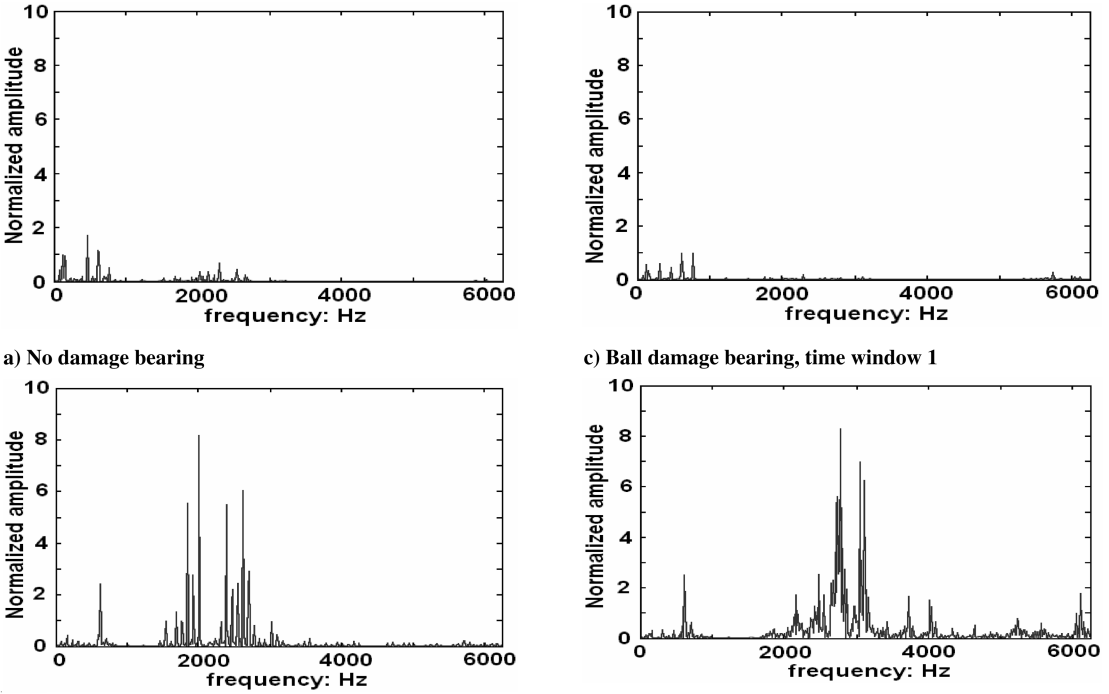

Fig. 5 Frequency spectra for different bearing cases.

indicate any type of damage. The wavelet plot in Fig. 7b represents the case 2 in which damage is located in the inner race at around 200 deg from the reference mark as indicated by the WVD in Fig. 6b. In this case, substantial vibration amplitudes can be found between the frequencies of 1500–3000 Hz. The results for the case of ball-element damage, as shown in Fig. 7d, depict larger vibration amplitudes than the previous three cases, as indicated by the significant darkening in the gray scale. Because the vibration frequencies in both the race and ball-element damage cases are all excited between the frequency ranges of 1500–6600 Hz, a comparison of the gray scale can provide information on relative vibration amplitudes, which can be used to relate to the levels of damage. Although the wavelet transform, in this case, seems to provide better insight in quantifying the damage in the bearing, it

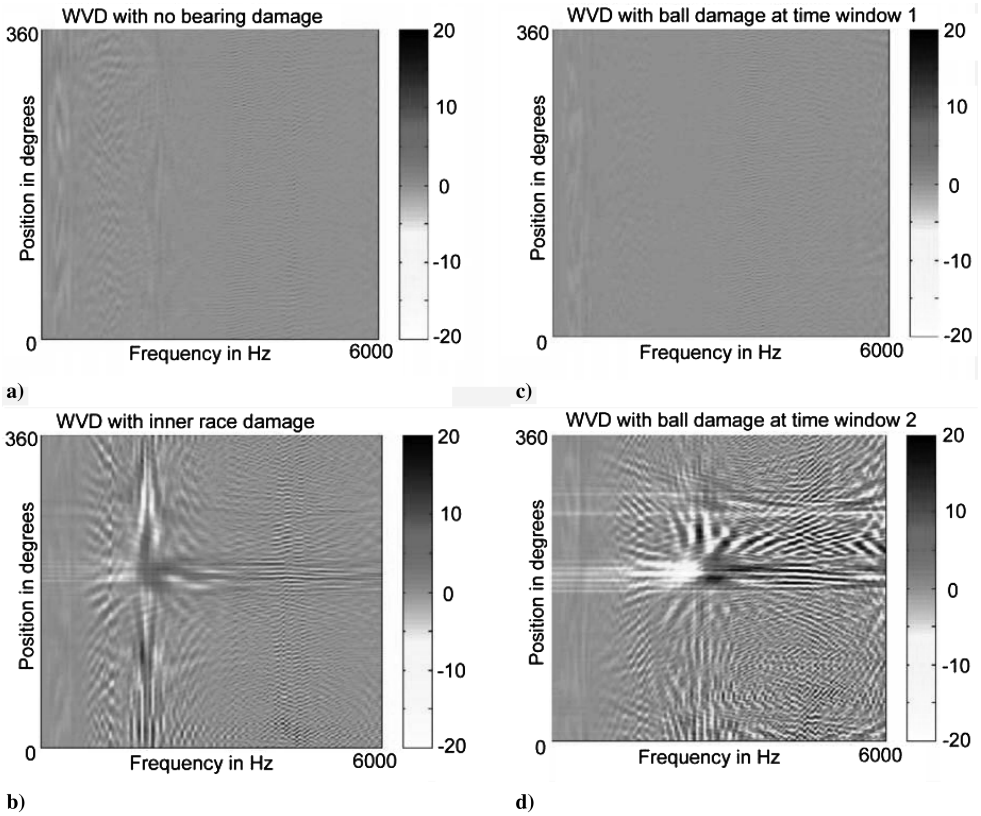

Fig. 6 Wigner–Ville distributions of vibration signal for different bearings.

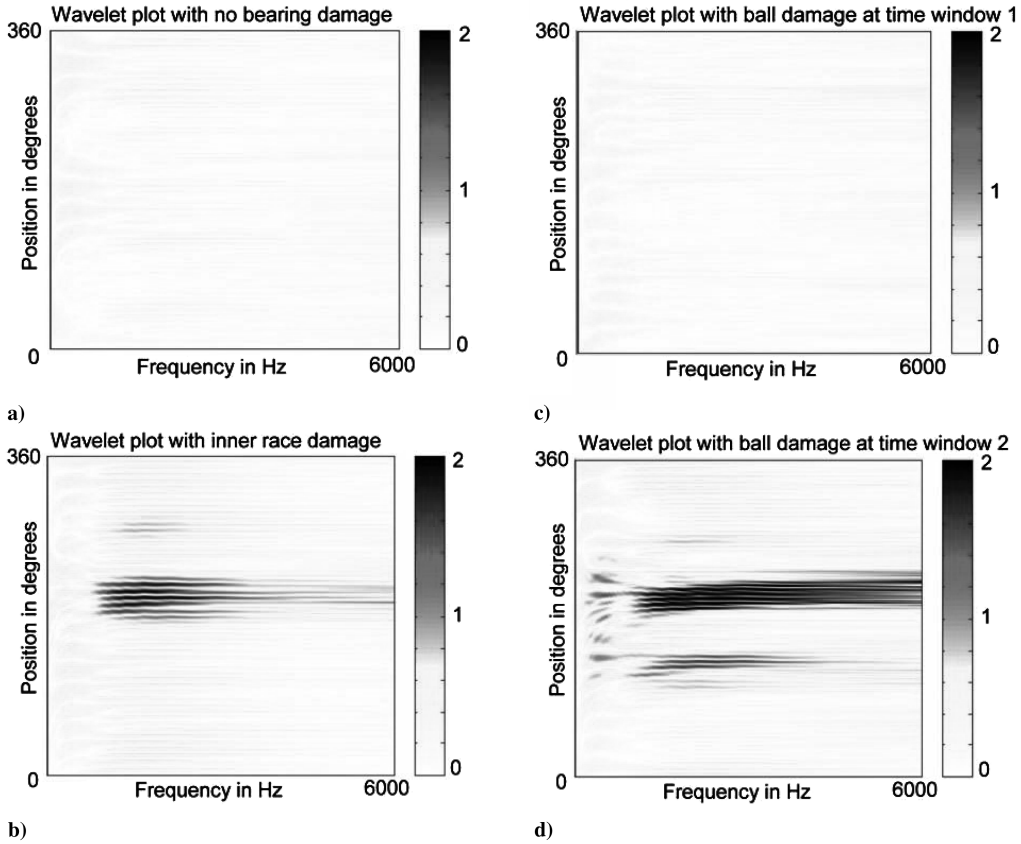

Fig. 7 Wavelet transforms of vibration signal for different bearings.

cannot provide a good indication of the type of damage in the bearing.

Because of the chaotic nature of the motion of the ball element, a modified Poincaré map [12,13] based on chaotic vibration theory with data averaging over 2000 revolutions is used to detect and quantify the damage at both the inner race (case 2) and the ball element (case 3). The use of a large data set of vibration information, namely, for 2000 revolutions, will ensure ample opportunities for the damaged location at the ball element to contact with the inner/outer races. In this study, modified Poincaré maps using both shaft speed and relative cage speed are used based on the following reasons: The shaft speed modified Poincaré map represents the dynamic characteristics of the shaft during one complete shaft (inner race) revolution. For the case of inner race damage, the vibration due to the race damage can be detected by the sudden increase in vibration amplitude during one shaft revolution and the damage location on the shaft/inner race can be determined by the relative angular position with the shaft triggering/timing mark. The relative cage speed modified Poincaré map represents the dynamic characteristics of the shaft during one complete revolution of the ball cage relative to the inner race. In other words, the modified Poincaré map will represent the period for all the ball elements to travel over once a particular location at the inner race. For bearing with inner race damage, such time period will include the period for interactions of all ball elements with the race-damaged area such that the number of vibration peaks will be equal to the number of ball elements. The existence of such multiple peaks phenomena can provide further confirmation of the inner race damage detection.

Figure 8 shows the modified Poincaré maps of both averaged and maximum vibrations (measured in volts) for 2000 shaft revolutions at a shaft speed of approximately 80 Hz (based on the optical encoder for each shaft revolution to minimize the effects of the variations of speed due to the electric motor). Figure 8a shows the modified Poincaré map for averaged vibrations with no damage. Results from the inner race damage and the ball-element damage cases are given in Figs. 8b and 8c, respectively. Note that the modified Poincaré map with the inner race damage given in Fig. 8b shows a very substantial increase in vibration amplitude at the 9 o'clock position (relative to the reference mark at the positive x axis). Such a large increase in the vibration amplitude not only indicates bearing damage, but it also provides a more definite quantification of the damage. The modified Poincaré map due to ball-element damage given in Fig. 8c shows some increase in vibrations when compared to the one with no damage, but does not provide a good indication of the ball-element failure. The plots of maximum vibrations show a very significant increase in vibration amplitudes for the ball damage case in Fig. 8f, but are not as pronounced in the inner race damage case in Fig. 8e.

Further investigation showed that using the cage speed (instead of the shaft speed for the modified Poincaré map) provides a better identification and quantification of the bearing damage. Figure 9 shows the results of both averaged and maximum vibrations for all three cases at the cage speed of approximately 2.5 times the shaft speed (based on the optical encoder for each cage revolution). Note that in Fig. 9b, the vibration signature displays eight peaks around the bearing circumference as a result of the eight ball elements rolling past the inner race damaged location during one revolution of the cage. In this case, not only is the damage at the inner race easier to identify, but it can also be readily quantified by the change in peak vibration amplitudes when compared to the baseline undamaged case in Fig. 9a (about three times larger). Results from the ball-element damage, as shown in Fig. 9c, are significantly higher than those with no damage as shown in Fig. 9a. The results shown in Figs. 9d–9f display a much more distinct increase in vibrations for both the race damage and ball damage cases. Based on examinations of the plots given in Fig. 9, one can conclude that the inner race damage can be better detected by the averaged vibration map, whereas maximum vibration map will be better for identifying the ball-element damage. However, due to the chaotic motion of the ball elements, the statistical averaged vibrations will provide a better estimation of the level of

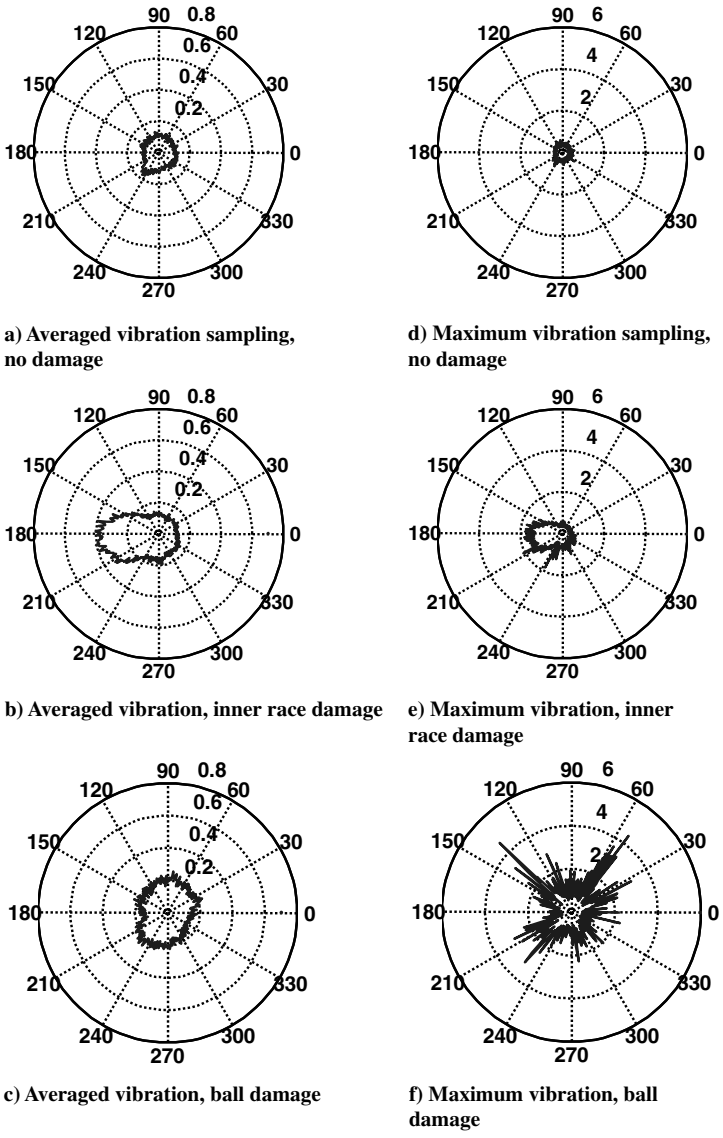

a) Averaged vibration sampling, no damage

d) Maximum vibration sampling, no damage

b) Averaged vibration, inner race damage

e) Maximum vibration, inner race damage

c) Averaged vibration, ball damage

f) Maximum vibration, ball damage

Fig. 8 Modified Poincaré maps, shaft speed.

damage in the bearing, as discussed in a recent publication by the author [14].

V. Conclusions

In conclusion, the study shows that, in the case of bearing race damage, where interactions with the damage area occur in a periodic manner during shaft rotation, vibration signals resulted from the damage interactions can usually be found within a typical sampling window. The four selected online procedures, the time domain analysis, the frequency domain analysis, the joint time-frequency analysis, and the modified Poincaré map, can be effective in various degrees in identifying the existing damage. For the case with ball-element damage, the vibration signals are chaotic in nature due to the unpredictable rotational patterns of the ball elements and interactions with the damage in the ball element may not occur within the particular data sampling period. As a result, the damage cannot be detected by the traditional time-frequency procedures, whereas the modified Poincaré map procedure using a relatively large amount of sampling data can be effective in identifying such damage.

Specific conclusions based on the results of this study can be summarized as follows:

1) The use of time signature data can provide information on the overall increase of vibration amplitudes without any specific indications of the type or location of the damage.

2) The use of frequency spectrum analysis can provide good indications of the component damage by the existence of large side band components. However, the vibration spectrum can sometimes be difficult to interpret, and it does not provide specific information on the types and location of the damage.

3) The Wigner–Ville distribution can provide a relatively good indication of the type and location of the damaged component, but it does not provide a very good estimation of the level of the damage. Using the wavelet transform in conjunction with the WVD can provide a better estimate of the level of damage in the bearing.

4) The use of the modified Poincaré map can provide a good identification of the ball element and inner race damages in the bearing system. The statistical approach based on time data taken over a longer period of time can ensure interactions between the damaged location on the ball element with the inner/outer races of the bearing during the sampling window. The level of damage can generally be determined by the amplitudes of the peaks displayed in the modified Poincaré map.

5) Using the modified Poincaré map with the shaft speed, the location of the race damage relative to the shaft reference/timing triggering mark can be determined. When the modified Poincaré map with cage speed is used, the vibration characteristics of each ball element rolling over the inner race damage area will be displayed, with number of peaks equal to the number of ball elements, for damage confirmation and quantification. The existence of such

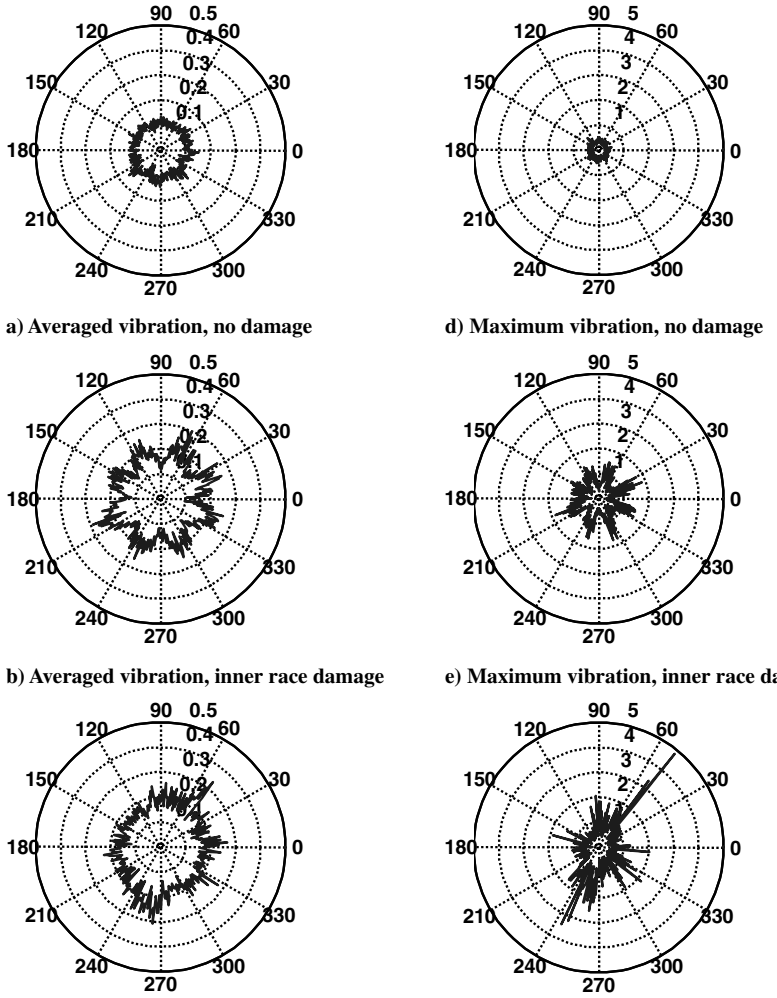

a) Averaged vibration, no damage

d) Maximum vibration, no damage

b) Averaged vibration, inner race damage

e) Maximum vibration, inner race damage

c) Averaged vibration, ball damage

f) Maximum vibration, ball damage

Fig. 9 Modified Poincaré maps, cage speed.

multiple peaks phenomena can provide further confirmation of the inner race damage detection.

6) Using the modified Poincaré map with average vibration amplitudes, a data bank on the relationships between vibration amplitudes and various degrees of bearing damage can be established to provide upper limits for real time bearing life prognosis. The results on such statistical analysis based on a large quantity of industrial bearings will be reported in a forthcoming paper.

References

[1] Bamberger, E. N., Harris, T. A., Kacmarsky, W. M., Moyer, C. A., Parker, R. J., Sherlock, J. J., and Zaretsky, E. V., *Life Adjustment Factors for Ball and Roller Bearings*, ASME, New York, 1971, pp. 8–14.

[2] Hadden, G. B., Kleckner, R. J., Ragen, M. A., and Sheynin, L., "Steady State and Transient Thermal Analysis of a Shaft Bearing System Including Ball, Cylindrical and Tapered Roller Bearings," SKF Research Report for Computer Program AT81Y003 SHABERTH, submitted to NASA Lewis Research Center, May 1981.

[3] Lundberg, G., and Palmgren, A., "Dynamic Capacity of Rolling Bearings," *Acta Polytechnica Scandinavica, Mechanical Engineering Series*, Vol. 1, No. 3, 1947, p. 7.

[4] Choy, F. K., Polyshchuk, V., Zakrajsek, J. J., Handschuh, R. F., and Townsend, D. P., "Analysis of the Effects of Surface Pitting and Wear of the Vibrations of a Gear Transmission System," *Tribology International*, Vol. 29, No. 1, 1996, pp. 77–83.

[5] Choy, F. K., Huang, S., Zakrajsek, J. J., Hanschuh, R. F., and Townsend, D. P., "Vibration Signature Analysis of a Faulted Gear System," *Journal of Propulsion and Power*, Vol. 12, No. 2, March–April 1996, pp. 289–295.

[6] McFadden, P. D., "Detecting Fatigue Cracks in Gears by Amplitude and Phase Demodulation of the Meshing Vibration," *Journal of Vibration, Acoustics, Stress, and Reliability in Design*, Vol. 108, No. 2, April 1986, pp. 165–170.

[7] McFadden, P. D., and Wang, W. J., "Time Frequency Domain Analysis of Vibration Signal for Machinery Diagnostics- The Wigner-Ville Distribution," University of Oxford, Report No. OUEL-1891, 1991.

[8] Forrester, B. D., "Analysis of Gear Vibration in the Time Frequency Domain," *Proceedings of the 44th Meeting of the Mechanical Failure Prevention Group*, Vibration Institute, Willowbrook, IL, Feb. 1990, pp. 225–234.

[9] Polyshchuk, V., "Detection and Quantification of the Gear Tooth Damage from the Vibration and Acoustic Signatures," Ph.D. Dissertation, Univ. of Akron, Akron, OH, May 1999.

[10] Misiti, M., Misiti, Y., Oppenheim, G., and Poggi, J., "Wavelet Toolbox for Use with Matlab," *Matlab Toolbox User Guide*, The MathWorks, Inc., Natick, MA, 1997.

[11] Mallat, S., *A Wavelet Tour of Signal Processing*, Academic Press, New York, 1998.

[12] Ehrich, F. F., "Some Observations of Chaotic Vibration Phenomena in High-Speed Rotordynamics," *Journal of Vibration and Acoustics*, Vol. 113, Jan. 1991, pp. 50–57.

[13] Moon, F. C., *Chaotic Vibrations*, Wiley-Interscience, New York, 1987.

[14] Choy, F. K., Zhou, J., Braun, M. J., and Wang, L., "Vibration Monitoring and Damage Identification of Faulty Ball bearings," *Journal of Tribology*, Vol. 127, Oct. 2005, pp. 776–783.

C. Tan
Associate Editor